

Kriging of Airborne Gravity Data in the Coastal Areas of the Gulf of Mexico

Hongzhi Song, Alexey L. Sadovski, Gary Jeffress

Conrad Blucher Institute, Texas A&M University-Corpus Christi, Corpus Christi, USA
Email: Alexey.sadovski@tamucc.edu

Received July 2013

ABSTRACT

This paper deals with the application of kriging technique to find the continuous map of gravity on the geoid in the coastal areas and to evaluate its precision.

Keywords: Gravity; Kriging; Geoid; Map; Statistics

1. Introduction

By using satellites, scientists discovered the long wave (large scale) geoid for the Earth (Seeber, 2003; Drinkwater et al., 2003) [1], but its resolution is not sufficient for orthometric height determination from GPS when it comes to the relatively small scale and/or local events such as flooding. This was the case after flooding created by storm surges from hurricanes Katrina, Rita (2005), and Ike (2008) in the coastal areas of the Gulf of Mexico. So, there is a need to develop method(s) and model(s) of the geoid determination at the local level, based on local observations of gravity, and complemented by observations of gravity from the air and space.

In principle, there is a need for gravity g at every point of the Earth's surface. Gravity is continuously changing, and it reflects the results of Earth's phenomena, such as tropic storm, hurricane, earthquake, early tides, variation in the atmosphere density, etc. Gravity also alters when only a small change happened in the constructions and the density of materials beneath the constructions. But having gravity data provided everywhere on the Earth is totally impossible in reality. To predict values of a random unsampled area from a set of observations is needed. It is well known that the kriging method is not the best approach to predict free-air gravity anomalies, but in this paper, we assume that the kriging method is a better approach than other methods for prediction of gravity based on the airborne data provided by National Geodetic Survey (NGS). The result we still have a confidence in the kriging method is that the kriging method can estimate the prediction error to assess the quality of a prediction. This function makes the kriging method with a big difference from other methods.

2. Data

Data used in this chapter is airborne gravity data of the Gravity for the Redefinition of the American Vertical Datum (GRAV-D) project which was released by NGS [2]. **Table 1** lists the nominal block characteristics, and details can be founded in *GRAV-D General Airborne Gravity Data User Manual*. Four blocks (Block CS01, CS02, CS03 and CS04) data (**Figure 1**) were chosen to be interpolated.

The total sample size (four blocks together) is 389578, and the gravity values range between 975480 mGal and 977490 mGal. Keep in mind, the standard gravity is 980665 mGal. The airborne gravity data was fixed by using free-air reduction and by the international gravity formula [3].

3. Kriging of Gravity on the Geoid

The kriging method here was conducted by using ArcGIS 10.1—Spatial Analyst and Geostatistical Analyst. There are six different types of kriging in Geostatistical Analyst tools. The most common types are ordinary kriging and universal kriging, which were chosen to be used in this study. The simple kriging method is also

Table 1. Nominal data characteristics.

Characteristic	Nominal Value
Altitude	20,000 ft (~ 6.3 km)
Ground speed	250 knots (250 nautical miles/hr)
Along-track gravimeter sampling	1 sample per second = 128.6 m (at nominal ground speed)
Data Line Spacing	10 km
Data Line length	400 km
Cross Line Spacing	40-80 km
Cross Line Length	500 km
Data Minimum Resolution	20 km

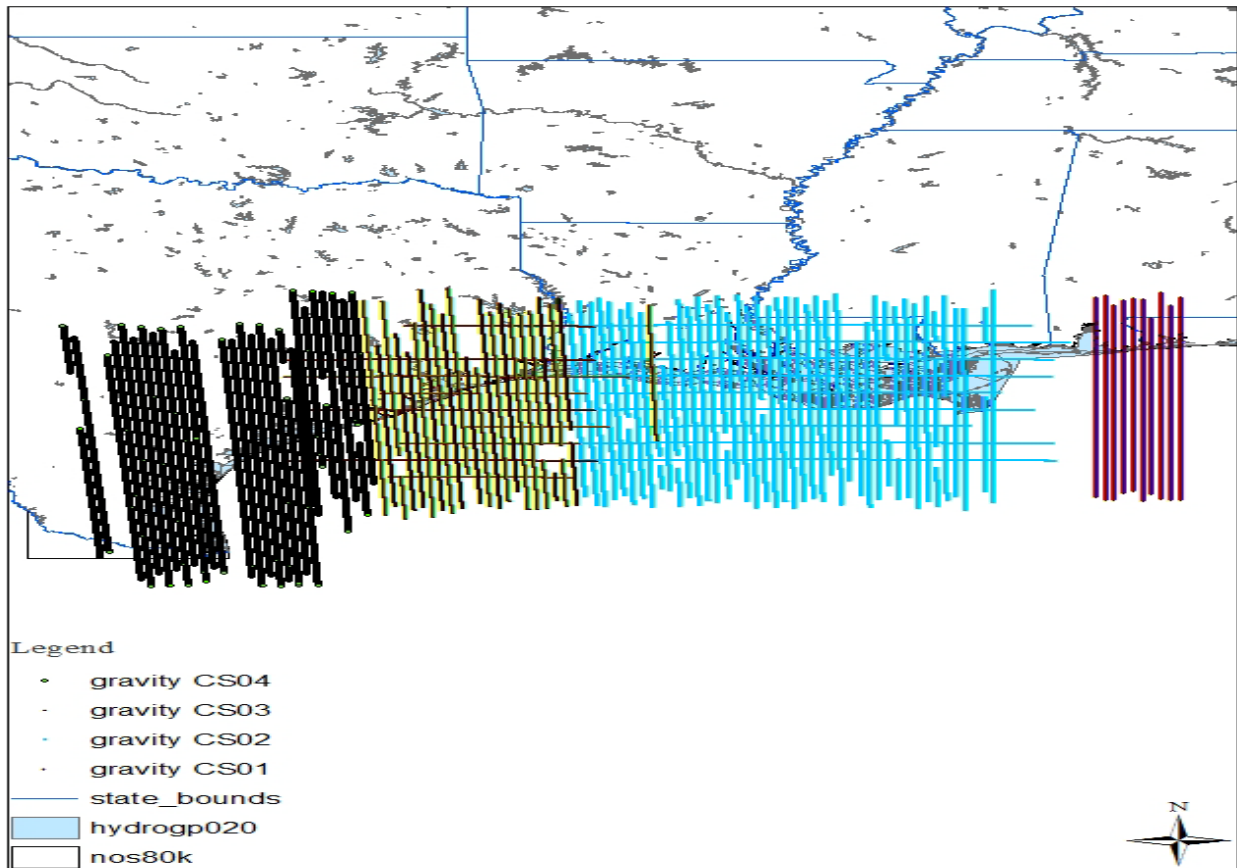


Figure 1. Tracks and locations of data of airborne gravity.

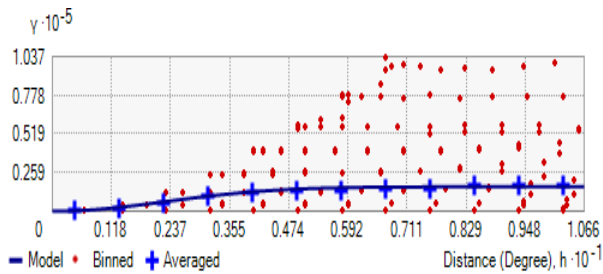


Figure 2. The average semivariogram values.

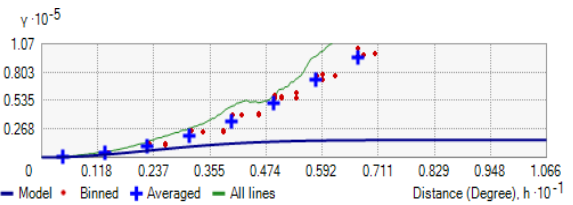


Figure 4. Semivariogram with showing search direction. The tolerance is 45 and the bandwidth (lags) is 3. The local polynomial shown as a green line fits the semivariogram surface in this case.

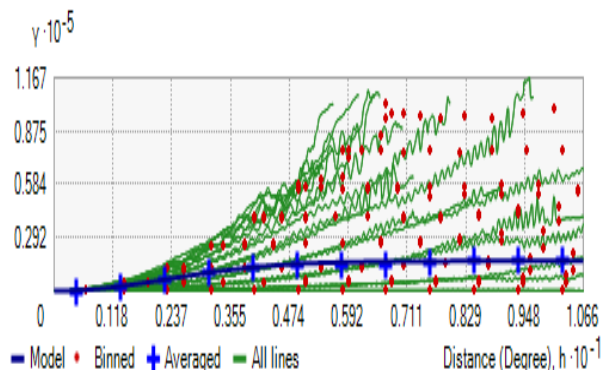


Figure 3. Semivariogram with all lines (green lines) which fit binned semivariogram values.

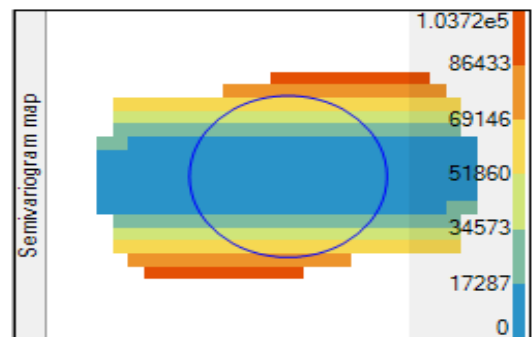


Figure 5. A semivariogram map. The color band shows semivariogram values with weights.

quite common, but it requires that the data should have normal distribution. Thus, the simple kriging method was not applied in this study. There are three major components—the spatial autocorrelation component (known as semivariogram), a trend, and a random error term. These three components are the key to lead to different types of the kriging methods. The simple equation represents the

kriging method is: $z_s = \sum_{i=1}^n z_i w_i$, where z_s is the estimated value for an unsampled location s ; z_i is the known value at the control point i ; w_i represents the weight applied to sample values associated with the control point i ; n is the number of sample points used in the estimation.

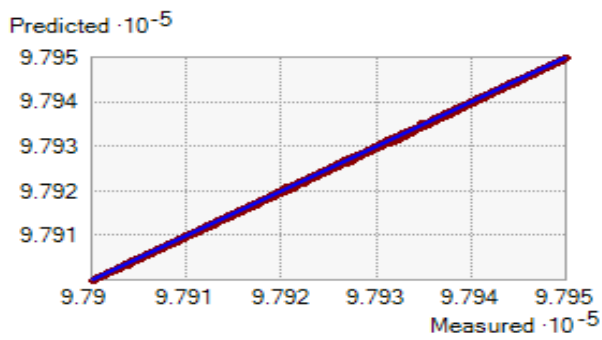
The averaged semivariogram values on the y-axis (in mgal^2), and distance (or lag) on the x-axis (in degree). Binned values are shown as red dots, which are sorted the relative values between points based on their distances and directions and computed a value by square of the difference between the original values of points; Average values are shown as blue crosses, which are generated by binning semivariogram points; The model is shown as blue curve, which is fitted to average values. Model: $28.118 * \text{Nugget} + 16437 * \text{Stable} (5.53,2)$; Model: $28.118 * \text{Nugget} + 16437 * \text{Gaussian} (5.53)$.

The predicted, error, standard error, and normal QQ plot graphs are plotted respectively in **Figures 6(a)-(d)**. The predicted graph shows how well the known sample

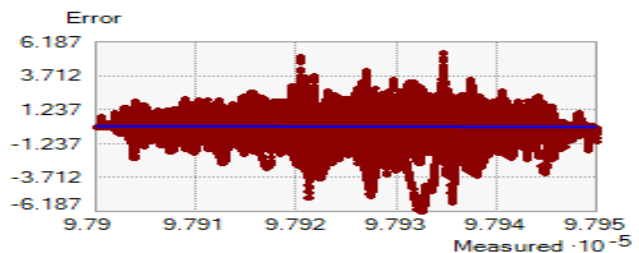
value was predicted compared to its actual value. The regression function in **Figure 6(a)** is $f(x) = 0.9999x + 125.1751$. By visually analyzed the graph, the regression function is closely aligned with the reference line. Therefore, it is well predicted.

The error graph shows the difference between known values and predictions for these values. The error equation in **Figure 6(b)** is $y = 10.00001x + 127.1751$. The standardized error graph shows the error divided by the estimated kriging errors. The standardized error equation in **Figure 6(c)** is $y = 10.00002x + 22.9974$. The normal QQ plot of the standardized error **Figure 6(d)** shows how closely the difference between the errors of predicted and actual values align with the standard normal distribution (the reference line). **Figures 7 and 8** demonstrate the prediction and standard error map by using the ordinary kriging with stable and Gaussian techniques.

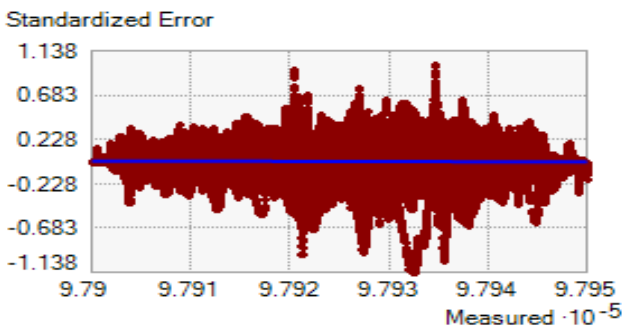
Trend analysis was presented in **Figure 9**. There is no trend exists because the curve through the projected points is flat (as shown by the light blue line in the **Figure 9**). A slight downward curve as shown by the red line in **Figure 9** is through the projected points on ZY plane, which suggests that it may have a trend exist in gravity on the geoid data. Therefore, de-trend is conducted before the universal kriging process in order to prevent biased the analysis. Because the curve shown on ZY plane is not obvious, the de-trend approach is chosen



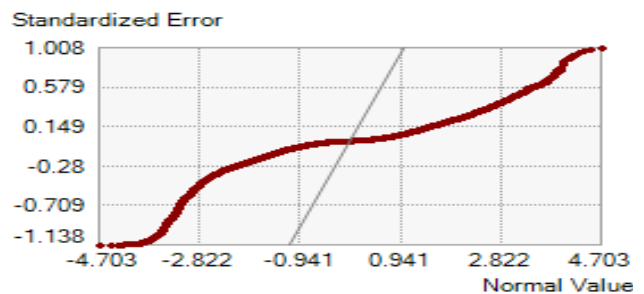
(a)



(b)



(c)



(d)

Figure 6. Cross validation of the ordinary kriging.

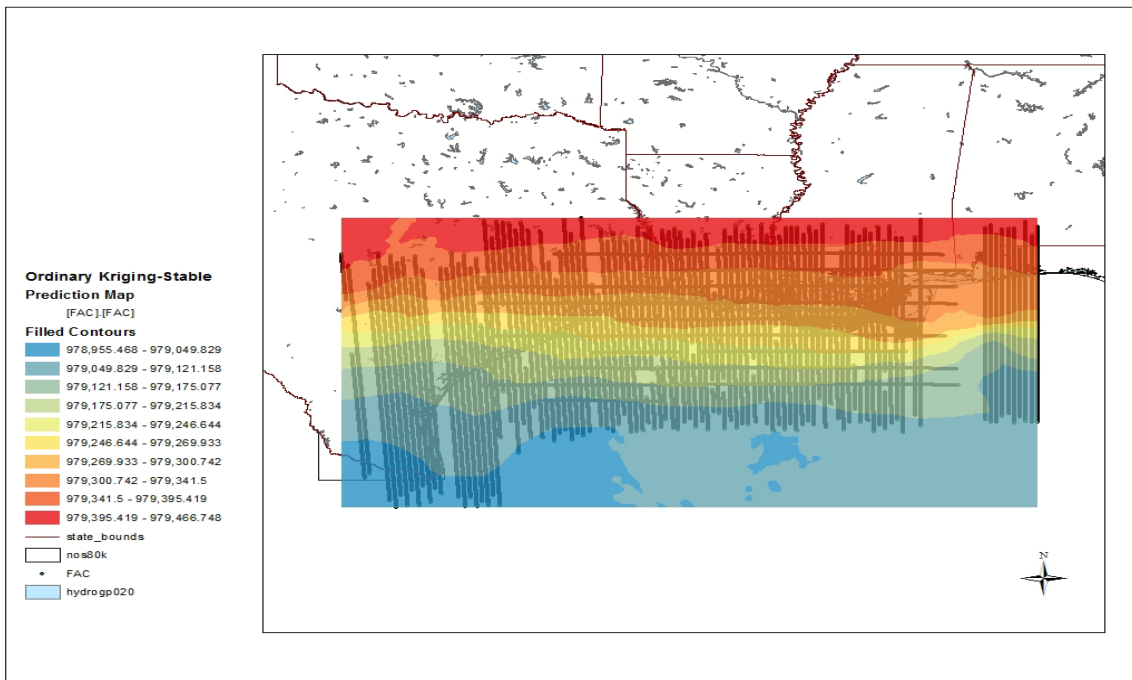


Figure 7. The ordinary stable and Gaussian kriging predictions map.

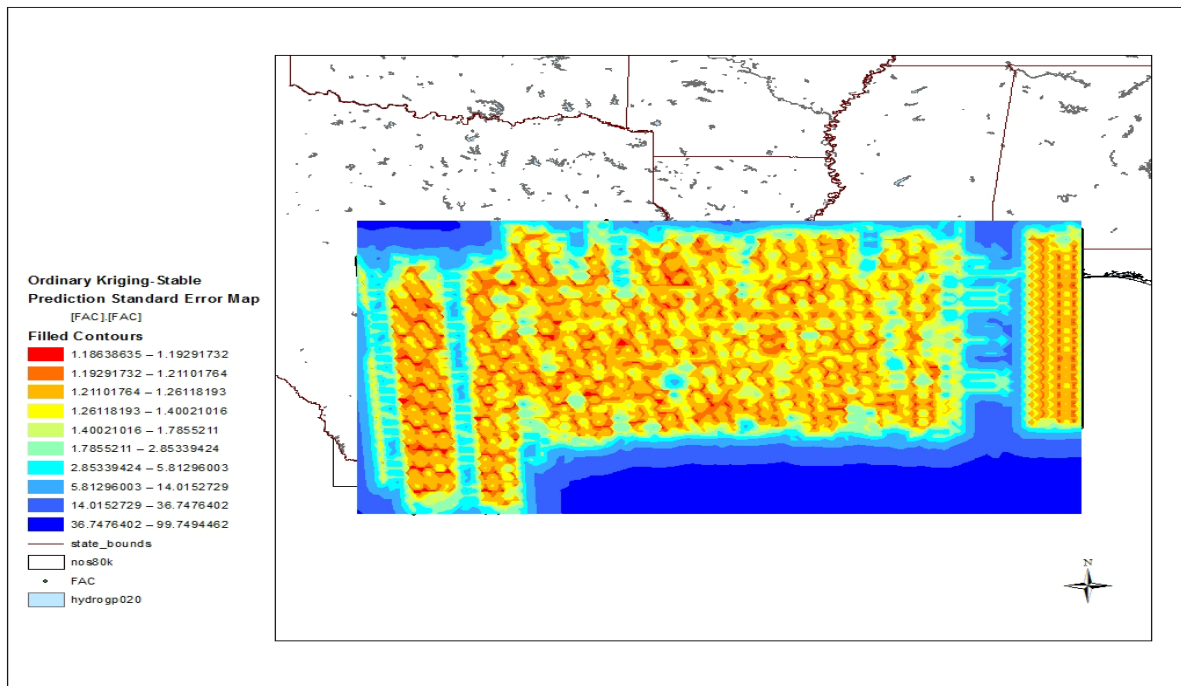


Figure 8. The ordinary stable and Gaussian kriging prediction standard error map.

to remove the trend order as constant. The process was conducted in ArcGIS 10.1 by using Geostatistical Analyst. Results of the universal kriging with either the stable technique or the Gaussian technique were shown as exact the same as results of the ordinary kriging.

Legend: Grid (XYZ): Number of Grid Lines $11 \times 11 \times$

6; Projected Data: YZ plane (Dark Blue), ZY plane (Yellow), XY plane (Peony Pink); Trend on Projections: YZ plane (Light Blue), XZ plane (Red); Axes (Black).

A better interpolation method should have a smaller RMS. Due to no difference between the ordinary kriging and universal kriging in this case; statistical results were

Table 2. Statistics.

RMS Standardized	0.1084
Mean Standardized	0.0007
Average Standard Error (ASE)	5.5060
Root Mean Square (RMS)	0.5918
Difference between RMS and ASE	4.9142
Difference in Percentage	89.25%

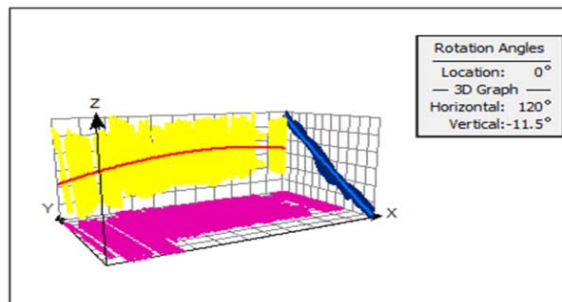


Figure 9. Trend analysis of gravity on the geoid.

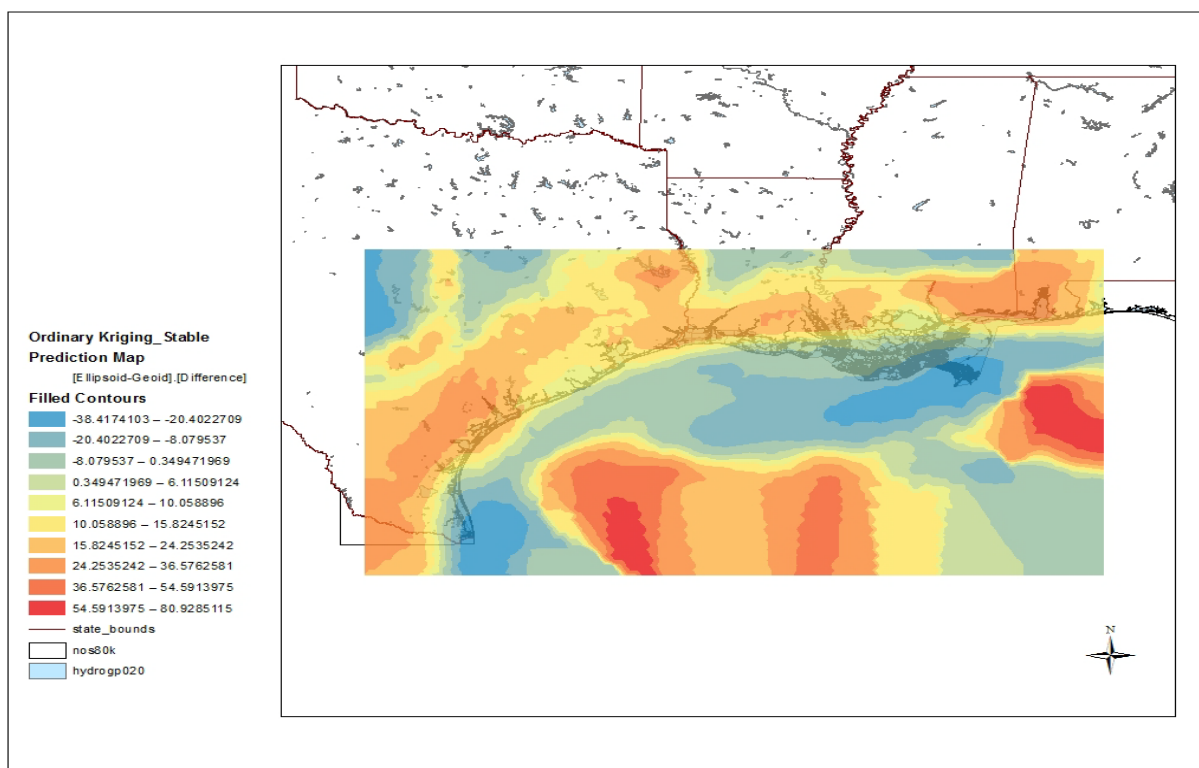


Figure 10. The ordinary kriging predictions map of gravity on the geoid along Gulf of Mexico coast.

the same which listed in **Table 2**. The prediction error mean is 0.0038 mGal. As 1 meter increased in altitude, the gravity is decreased by 0.3086 mGal. With simple conversion, the accuracy of prediction is approximately 0.0123 meters. Namely, it is around 1.23 cm, which was expected.

REFERENCES

[1] M. R. Drinkwater, R. Floberghagen, R. Haagmans, D. Muzi and A. Popescu, “VII: CLOSING SESSION: GOCE: ESA’s First Earth Explorer Core Mission,” *Space Science Reviews*, Vol. 108, No. 1-2, 2003, pp. 419-432.

[2] GRAV-D Science Team, “GRAV-D General Airborne Gravity Data User Manual,” Theresa M. Diehl, Ed., Version 1, 2011. http://www.ngs.noaa.gov/GRAVD/data_cs01.shtml

[3] X. Li and H. J. Götze, “Tutorial Ellipsoid, Geoid, Gravity, Geodesy, and Geophysics,” *Geophysics*, Vol. 66, No. 6, 2001, pp. 1660-1668. <http://dx.doi.org/10.1190/1.1487109>

[4] B. Hofmann-Wellenhopf and H. Moritz, “Physical Geodesy,” 2nd Edition, Springer Wien, New York, 2006. <http://dx.doi.org/10.1023/A:1026104216284>